Comparison of near wind farm wake measurements from scanning lidar with engineering models

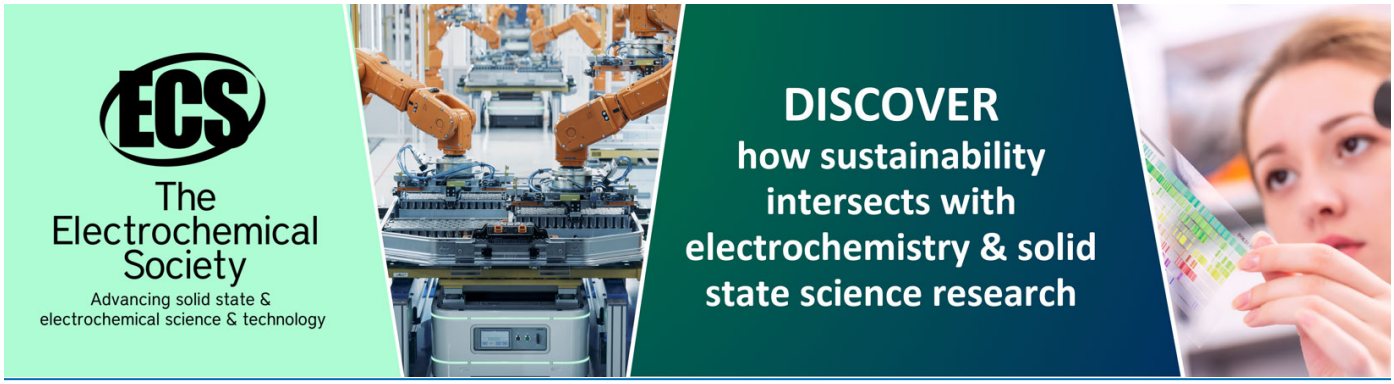

Comparison of near wind farm wake measurements from scanning lidar with engineering models

A Anantharaman[1], G Centurelli[1], J Schneemann[1], E Bot[2] and M Kühn[1]

[1] ForWind, Institute of Physics, University of Oldenburg, Küpkersweg 70, 26129 Oldenburg, Germany
[2] TNO Energy Transition, Westerduinweg 3, 1755 LE, Petten, The Netherlands

E-mail: arjun.anantharaman@uni-oldenburg.de

Abstract. The presence of offshore wind farms causes downstream regions of reduced wind velocity, i.e. wind farm (cluster) wakes, which can affect the power of wind farms downstream. Engineering models are now being used to simulate the effects of these wakes, and an important requirement for model validation is a comparison with full-field measurements. Our objective in this paper is to parametrize and validate two engineering wake models with long-range lidar measurements. We use a long-range scanning Doppler lidar to scan the near wake region of a 400 MW offshore wind farm and compare the wind velocities in the wake to the outputs of two engineering models: FarmFlow and *flappy*. We adapt FarmFlow to solve the flow in highly unstable atmospheres by modifying the boundary conditions, which enables the comparison of velocity profiles behind the farm. The models perform qualitatively well in predicting the wake deficit and shape close to the farm and at lower heights. They predict higher wake losses within the farm when compared to production power data in a strongly unstable atmospheric case. However, the current analysis is limited due to the lack of inflow measurements for model initialization, compounded by limited data availability. We discuss the possibilities and limitations of long-range scanning lidar data for cluster wake model validation and the need for inflow measurements for model initialization. We conclude that with detailed inflow measurements, scanning long-range lidars could serve as a good tool for the validation of wind farm wake models.

1. Introduction

Engineering wake models for wind farm resource assessment have primarily focused on the representation of the wakes of single wind turbines and inner wind farm effects. The combined wakes of all wind turbines in a wind farm (called cluster wakes or wind farm wakes) have been shown to adversely affect the power production of downstream wind farms in specific meteorological situations [1]. A validated representation of cluster wake effects in engineering models can reduce uncertainty in resource assessment for future offshore wind farm projects.

Cluster wakes have been studied for several years using spaceborne synthetic aperture radar (SAR) [2], Doppler radar [3], research aircrafts [4], long-range lidar [1], met masts [5] and wind farm operational data [6]. Platis et al. found that cluster wakes can last more than 50 km downstream in stable atmospheric conditions [4], while Schneemann et al. proved an effect of cluster wakes on the power of a downstream wind farm lasting 55 km in stable and weakly unstable atmospheric conditions [1].

Large eddy simulations [7] and mesoscale simulations with e.g. the Weather Research and Forecasting model [8], while covering large areas offshore, are computationally expensive. The industry has thus continued to depend on analytical wake models for resource assessment, due to lower computational costs and also robustness for the calculation of the wind farm Annual Energy Production (AEP).

Several engineering wind turbine wake models have been used to model inner wind farm effects [9]. Recently, the focus of engineering wake models has shifted to the region behind wind farms, to include large scale effects such as wind farm wakes [6, 10]. Proper validation of large scale wind farm wake modelling is still a challenge since accurate measurement data is rarely available.

Traditional engineering models such as the Park model [11] underestimate the wake deficit behind large offshore wind farms when validated with the production data of a downstream wind farm. Applying a turbulence optimisation brought the Park model closer to a realistic representation of the wind farm wake. However, possible influences of the coast and uncertainties due to the indirect validation with wind farm production data have to be considered [6]. Parameterization of engineering wake models with a direct validation of the wind farm wake flow, especially in varying atmospheric stabilities, is still pending.

The objective of this paper is the tuning and validation of two engineering wind farm wake models with lidar measurement data. We achieve this goal by a) using a long-range scanning Doppler lidar to scan the wake region up to 8 km downstream of a 400 MW offshore wind farm in the German North Sea, and b) comparing the simulations of the wind farm wake from the two engineering models FarmFlow and *flappy* to the measurements.

2. Methodology

2.1. Lidar measurements at the offshore wind farm Global Tech I

A Leosphere WindCube 200S lidar was operated on the Transition Piece (TP) of turbine GT 58 in the Global Tech I (GT I) wind farm in the German North Sea. The lidar on the transition piece is 24.6 m above the sea surface. Figure 1 shows the layout of GT I and a photograph of the lidar. GT I consists of 80 Adwen AD5-116 wind turbines with a total rated power of 400 MW. The turbines have a rotor diameter (D) of 116 m and a hub height of 90 m.

The lidar performed Plan Position Indicator (PPI) scans with a fixed elevation (δ) of 0.8 °in an azimuthal range of 150 °. This results in a range of heights from approximately 31 m until 135 m above the sea surface (including turbine thrust caused platform tilt). This enables comparisons of the velocities behind the farm at different heights. The lidar scan settings are summarized in Table 1.

Table 1. Utilized lidar scan settings for the Leosphere WindCube 200S

φ range (°)	$\Delta\varphi$ (°)	Scan time (s)	Range gates (m)
150	2	150	500:35:7990

The lidar scan output contains the raw line-of-sight (v_{LOS}) velocities across the scanned ranges and azimuth angles φ. We processed the raw lidar data from individual scans using the data density filter of [12]. The horizontal velocities

$$u = \frac{v_{\mathrm{LOS}}}{\cos(\varphi - \phi)\cos\delta} \tag{1}$$

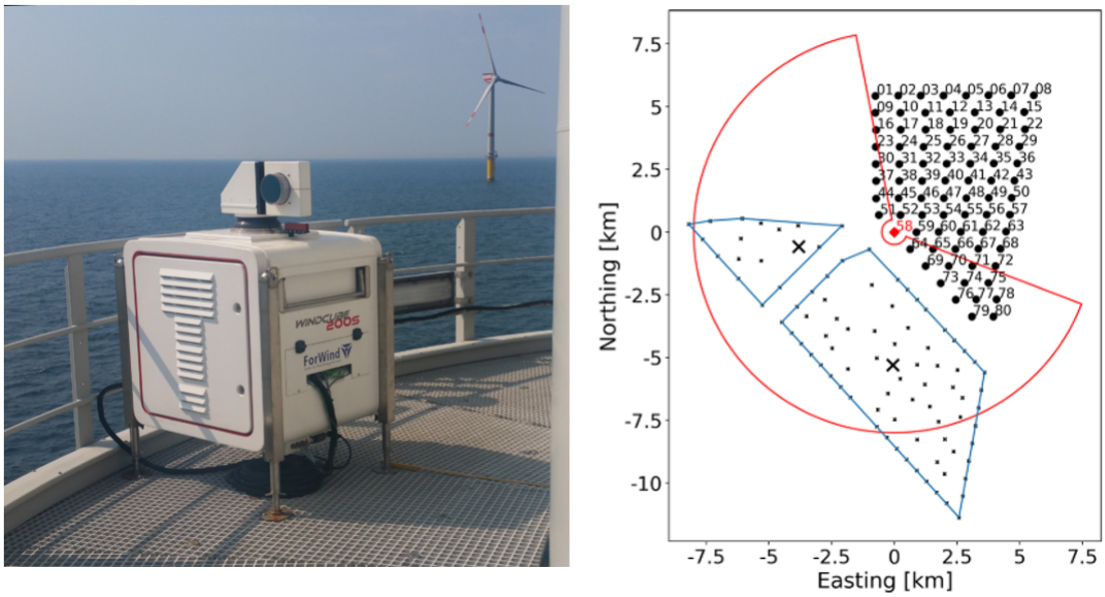

Figure 1. Leosphere WindCube 200S placed on the TP of a turbine in the Global Tech I wind farm (left). Scanned sector of the lidar measurements (right). Images taken from [1].

were obtained using the VAD fit method [13] with the assumption of a homogeneous wind field (uniform wind direction ϕ).

To compare the lidar measurements to the engineering models introduced in Sections 2.4 and 2.5, we consider two distances to compare the velocities within the wake, 20 D and 40 D downstream of the lidar and extending perpendicular to the wind direction. The lidar is located in the last row of turbines in the case of NNE wind, and the distance is calculated from the lidar location, along the direction of the wind. There is a hard target in the middle of the lidar scan resulting in a small blind sector. After the VAD fit, the result is a scatter of points as a function of range and azimuth. This was then interpolated over a uniform grid to fill in the missing data at longer ranges, as shown in Figure 2.

2.2. Lidar measurement uncertainties

The uncertainties for the lidar measurements can be divided into two categories: velocity and height uncertainties. The velocity derived from Equation (1) explicitly assumes a homogeneous wind direction. We did not account for the spatial wind direction changes within each scan. To reduce the effect of temporal wind direction changes, we selected a scenario where the wind direction was nearly constant ($28° \pm 1°$) throughout the lidar scan period. We corrected deviating measurement heights caused by wind turbine thrust induced platform tilt using the algorithm introduced by [14]. In addition to this, the curvature of the earth was also taken into account using Equation (2), where L_{range} is the lidar measurement distance and $R \approx 6378$ km is the radius of the Earth. The effective measurement height is given by Equation (3).

$$h_{\text{curvature}} = \sqrt{L_{\text{range}}^2 + R^2} - R \tag{2}$$

$$h_{\text{effective}} = h_{\text{lidar}} \pm h_{\text{tilt}} + h_{\text{curvature}} \tag{3}$$

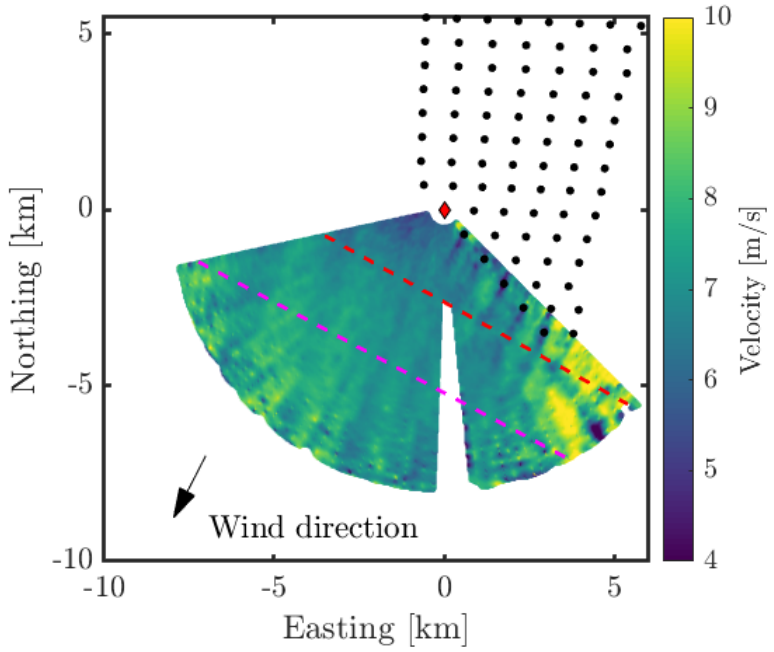

Figure 2. Lidar (red diamond) scan of the GT I wake, averaged over 20 minutes with the two cuts of 20 D (red dashed line) and 40 D (pink dashed line), perpendicular to the wind direction.

2.3. Atmospheric stability

We measured air pressure (Vaisala PTB330), temperature and relative humidity (Vaisala HMP155) simultaneously with the lidar scans and used the local sea surface temperature from a local measurement buoy to determine atmospheric stability at lidar height. This was input to the engineering models. The stability parameter used in the current study is the Monin-Obukhov length L, based on the the definition by [15]. We use this directly as an input in FarmFlow and account for the stability by tuning the wake decay and turbulence intensity in *flappy*. The Bulk Richardson number (Ri_b) is calculated first, from which the stability parameter ζ and consequently, L is determined using Equations (5)- (7), with the same assumptions as in [16].

$$Ri_{\mathrm{b}} = \frac{g}{T_{\mathrm{v}}} \frac{0.5 z_{\mathrm{TP}} \Delta\Theta}{u_{\mathrm{TP}}^2} \tag{4}$$

$$u_{10} = u_{\mathrm{meas}} \frac{\ln(\frac{z_{10}}{z_0}) - \Phi(\frac{z_{10}}{L})}{\ln(\frac{z_{meas}}{z_0}) - \Phi(\frac{z_{meas}}{L})} \tag{5}$$

$$\zeta = \begin{cases} \dfrac{10 Ri_{\mathrm{b}}}{1 - 5 Ri_{\mathrm{b}}} & Ri_{\mathrm{b}} > 0 \\ 10 Ri_{\mathrm{b}}, & Ri_{\mathrm{b}} \leq 0 \end{cases} \tag{6}$$

$$L = \frac{0.5 z_{\mathrm{TP}}}{\zeta} \tag{7}$$

For the case analysed in this paper, the atmospheric stability $L = -45$ m, which indicates a highly unstable atmosphere. However, it has to be noted that there is a high degree of uncertainty in using this stability to initialize the models, mainly due to the location of sensors. GT 58 is located far downstream, and in addition to being within the wake, it is representative of the stability at lidar height with the atmospheric measurements.

2.4. FarmFlow

FarmFlow is a wind farm wake modelling software developed by TNO. It solves the 3D parabolized Navier-Stokes equations using the k-ϵ model. It models the turbines as actuator disks and has been validated for several offshore wind farms [17]. The wakes from individual turbines are divided into three regions: the near-wake, the transition and the far-wake region. The k-ϵ model tends to overestimate the wake recovery in the near-wake region since it is time averaged and the turbulent kinetic energy production delay due to tip vortices is not accounted for. The turbulence production in the near-wake region is thus strongly limited in FarmFlow, adapted in the transition region and the normal k-ϵ model is applied in the far-wake.

FarmFlow was initially developed for simulating the wake interactions within a wind farm and hence accurately estimate its power production (thereby AEP). When inter-farm effects are considered, the flow is solved for larger distances behind the farm, where no turbine interactions exist. In neutral atmospheric conditions, this does not cause an issue, as the boundary conditions over each flow grid cell are unaffected. The boundary conditions for each grid cell (5.5 D in both width and height) are Neumann at the side and top walls, and Dirichlet at the bottom wall. The restriction is that mass conservation ensures a constant wake deficit in the cell. In very unstable atmospheric conditions, this restriction becomes unrealistic as the wake recovery is greatly enhanced by vertical mixing. One solution could be to increase the domain size to reduce the mass conservation effect, but that would result in very high computational times.

Results from a larger domain were thus first analyzed to get an estimate of the deficit at the boundary of a smaller domain. Hence, we updated FarmFlow so that the results from the smaller domain compared very well with the larger domain. This was achieved since the restriction from mass conservation allowed a reduction of the total wake deficit (not unrealistically high as before) from this estimated recovery rate at the boundary. The effect on power production was compared for two years of data on the Windpark Egmond aan Zee near the Dutch North Sea coast, and a small increase in power production (0.7%) was observed due to the enhanced recovery in the newer model, with no other noticeable changes in the outputs.

FarmFlow was optimized to provide velocity fields at any point by defining virtual met masts. This was set-up to coincide with the points considered in the lidar scans at 20 D and 40 D, with a height resolution of 14 m. To compare the velocity at a particular height, the closest matching height within FarmFlow was selected. This process was repeated for each point, since the uncertainty due to extrapolation errors (assuming a stability dependant velocity profile) was high. This results in a maximum error in height of 7 m, which is well within acceptable limits.

2.5. flappy

The Farm Layout Program in Python (*flappy*) is an in-house engineering model, developed by Fraunhofer IWES [18]. The turbines' interactions with the wind are represented according to analytical models that do not require the use of a grid for the solution. The wind properties at a turbine are sampled through a rotor model, this information is used by a wake model and a added turbulence intensity model, to characterize the wake generated by any single turbine in the simulation. Finally a superposition model takes care of composing the computed wakes with the undisturbed flow the simulation is initialized with. The combination of models we used is:

- Rotor model: averaged at 16 points in the rotor plane
- Wake decay model: Bastankhah Gaussian [19]
- Turbulence in the wind farm: Crespo and Hernandez [20]
- Wake superposition: Linear

While *flappy* offers also the possibility of representing the induction based wind farm blockage, the effects of this phenomenon on the current analysis were found to be negligible, thus we do not

included this type of model in the simulation performed. In *flappy*, the grid-less algorithm allows to directly sample the velocity field at any user defined point, this ensures to add no further uncertainty when comparing the model to the lidar scans due to mismatch in the sampling point locations. *flappy* is oriented to large time series processing, we performed a single simulation based on a very short time series created with the conditions found in the different lidar scans. The simulation is steady state, where any entry of the time series is processed independently from the others. For any timestamp, wind speed, wind direction, and ambient turbulence intensity must be defined. The wake modelling also require to set different coefficients modulating the wake recovery and the turbine added turbulence intensity decay. In our cases we defined a set of parameters that fit the atmospheric conditions found during the lidar scans.

2.6. Model initialization

The comparison of modeled wind fields and wind measurement data requires identical or at least similar flow situations. Therefore the initial conditions of the model, i.e. the inflow wind profile, atmospheric stability and turbulence intensity need to be known. In practice an undisturbed inflow measurement requires high efforts like a met mast, a second scanning lidar looking upstream or a lidar buoy. We did not have any upstream measurement available, therefore we used operational data of the upstream wind turbines in GT I to estimate the inflow. The power produced by the turbines in the entire first row (GT 1-8) was taken during the initial 20 minutes of the lidar measurements. This was done to account for the time the wind takes to reach the lidar location and the subsequent comparison distances of the velocity profiles from the inflow. A mean value of the front row turbines' power from the SCADA data was taken, and the inflow velocity was determined using this value (we reconstructed the power curve from the SCADA power data).

There were no measurements available for the turbulence intensity in the inflow. The FarmFlow update allowed solving the flow up to an Obukhov length of L=-200 m, and the turbulence intensity was increased until the flow could no longer be solved. The final values set within FarmFlow were 7.3 m/s for the free-stream wind speed and 14.5% for the turbulence intensity. To compare both models with the same inflow, the same conditions were set in *flappy*.

3. Results

3.1. Wake velocity comparison

We compare the lidar measurements with the simulated model outputs for a highly unstable atmosphere, along the specified downstream distances. Figure 3 shows the velocities in the wake of the GT I wind farm as a function of the distance perpendicular to the wind direction. Each point of the lidar measurements is at a different height, and despite a lack of information about the vertical wind profile, the match between the models and measurements is qualitatively good at 20 D. The models' behaviour at 40 D is more difficult to analyse as there are larger variations in the lidar measurements due to lower carrier to noise ratio. We noticed in the measurements that there was a small variation in the wind direction within the wake of the farm, which is quite complex to analyse and represent in the models. The qualitative match between measurements and models is, however, limited to the regions closer to the farm and at lower heights.

3.2. Comparison of model output to SCADA data

We compare the power output of the models to those of the turbines in the farm to evaluate the performance for intra-farm effects, in a highly unstable atmosphere. We use the freely available power and thrust curves of the NREL 5 MW reference turbine [21], which is very similar in performance to the Adwen turbine of the GT I farm. The power output of each turbine is

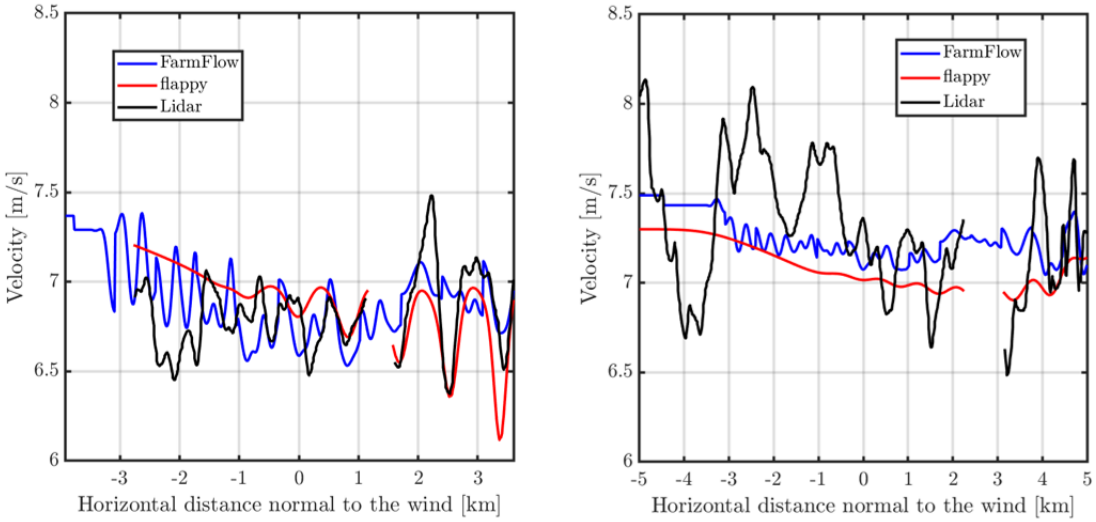

Figure 3. Comparison of the wake velocity profiles between the Lidar measurements (black, averaged over 20 min, as in Figure 2), FarmFlow simulations (blue) and *flappy* simulations (red), at 20 D (left) and 40 D (right) downstream and perpendicular to the wind direction.

normalized with the mean power of the first row as in Equation (8), and the deviation from the SCADA power is expressed as a percentage.

$$P_{\text{norm}} = \frac{P_{\text{turbine}}}{P_{\text{avg,firstrow}}} \tag{8}$$

For the power production analysis, we divide the farm into two regions: the front, which includes the first two rows, and the back which consists of the last few rows, as shown in Figure 4. We do this to determine how the models perform immediately after the front row, (which is used for the inflow velocity) and how the magnitude of error shifts the further we proced into the farm. The two regions for NNE wind are shown in Figure 4. The error is calculated for each turbine in both regions by calculating the deviation of the normalised model power from the normalised SCADA power, and then averaged for the front and back turbines. Both models underestimate the power in the front, possibly due to uncertainties in the method of determining the inflow velocity. However, this underestimation in the inflow power (< -5 %) is much lower than the overestimation in the downstream part of the farm (35 % in FarmFlow and 16 % in *flappy*). This is possibly due to the increased recovery set in the models to match the scan scenario of stability.

In addition to the progression of error through the farm, we also computed the overall error by averaging the individual error across all turbines. This might give biased results due to the averaging of outliers and thereby give the picture of better performance, so we compared the standard deviation of the power to assess the model performance within the farm. Both of these error quantifiers are summarised in Table 2. We found that both models overestimate the power production in the farm as a whole, and that *flappy* has lower errors in the mean and standard deviation when compared to SCADA power, indicating that it might better represent the intra-farm effects. Modifying the models to match the power was not performed since the velocities in the wake behind the farm were matched quite well, and the differences could be explained by the uncertainties in the inflow.

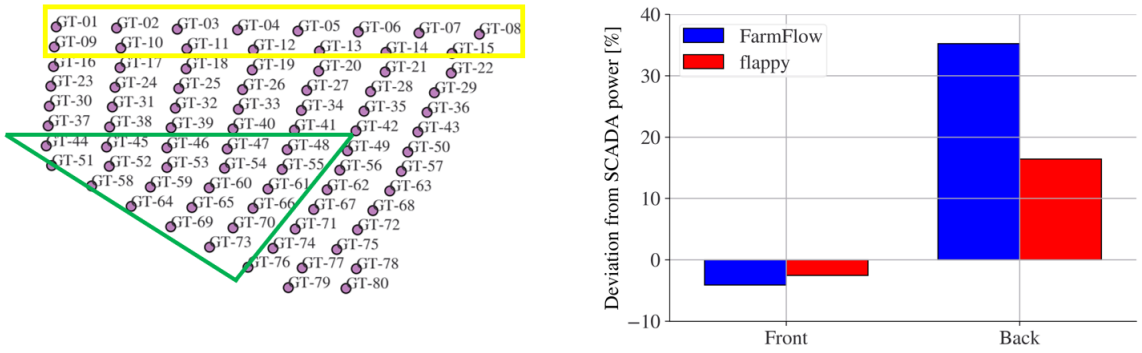

Figure 4. Division of the wind farm into the upstream (yellow frame) and downstream (green frame) regions (left). Percentage deviation of the mean power error predicted by FarmFlow and *flappy* when compared to the SCADA power data for the front and back regions (right).

Table 2. Comparison of the mean and standard deviation of the individual errors between FarmFlow and *flappy* when compared to the SCADA power data

Model	Mean error	σ (local effects)
FarmFlow	8.57 %	22 %
flappy	4.17 %	14 %

4. Challenges in the analysis

Parameterization of the engineering models based on lidar measurements led to a qualitative match closer to the farm and at lower heights, despite the lack of direct inflow measurements. The power output from the models was overestimated in the downstream part of the farm, possibly due to parameter settings in the models to match the highly unstable atmosphere. In addition to the aforementioned issues, there were also other challenges in the analysis, that hindered a comprehensive validation of the two models.

4.1. Time averaging and wind direction variability

We averaged the lidar scans (each scans takes 150 s) over a 20-minute period with a nearly constant wind direction. The averaging serves to smooth out or diffuse local turbulence. This does not have a noticeable effect when averaging out, but even longer averaging periods would be useful to compare the profiles to mesoscale models and smooth out any local effects that could affect wake formation.

4.2. Comparing the farm power output to the models

The average turbine output power in the first row is considered to represent the undisturbed wind farm inflow, but even within the first row, there are wind speed fluctuations that averaged out. This could be due to several reasons, and in some other cases we analysed, a clear variation in the inflow wind speed for each turbine was observed due to heterogeneities in the wind field.

4.3. Recommendations for future measurement campaigns
Based on our experience of analysing the available data of wind farm wakes and comparing the lidar measurements to models, we have the following recommendations for future campaigns with similar aims:

- A major source of uncertainty is the inflow. When the wake of the farm is under consideration for analysis, a detailed inflow description is necessary. While production data can be a good guide, an ideal campaign should have either a met mast or another lidar looking in front of the farm. An advantage in having a lidar is that heterogeneous wind fields can be identified and Range Height Indicator (RHI) scans can be performed to simultaneously determine the vertical wind profile.
- A comprehensive inflow measurement is not only limited to the free-stream velocity, but also the turbulence intensity and the atmospheric stability. Anemometers on a turbine could aid in real-time accurate TI values. In the current analysis, we utilised the difference in the temperature between the sea surface and the lidar heights, but this has two disadvantages: this is already inside the wake and the stability will also change with height. This remains a difficult measurement to perform accurately, especially offshore. One solution could be to account for the stability using the wind shear, or temperature sensors on the nacelle could be directly used.
- Ideally, the perfect farm layout for model validation should be symmetrical, or even better a standard layout, such as a square. This makes it easier for analysing multiple inflow directions, without having to account for local farm effects due to the geometry that might not be easily accommodated for in the models.
- Another goal could be that of a considerably longer measurement period which covers a variety of different atmospheric conditions in a statistically significant manner. A comparison of the power output to the Annual Energy Production (AEP) after the update of the models will be of great interest to wind farm operators.

5. Conclusions
The aim of the study was to parametrize engineering models to better represent the wake of an offshore wind farm by comparing the simulations to lidar measurements. We captured the near-wake of a large offshore wind farm using a long-range lidar, with elevated PPI scans. The velocities in the wake of this wind farm were compared to the output of the two engineering models, *flappy* and FarmFlow in a highly unstable atmosphere. Long-range remote sensing devices like a scanning lidar are well suited for the analysis of wind farm wakes. However, without a proper description of the inflow with additional (often more complex) measurements, a quantitative comparison to models is difficult.

We found that by changing the wake recovery parameter in analytical engineering models (like *flappy*) and by changing the boundary conditions in FarmFlow (RANS model), the models can predict the profile of the wind farm wake at 20 D, albeit closer to the farm and at lower heights. However, modifications in both models without definitive measurements of the atmospheric stability, turbulence intensity and the vertical wind profile causes an over prediction in the power in the downstream part of the farm, due to the enhanced recovery to match the highly unstable atmosphere. Wind farm wake model validation remains a challenging and important topic to address, and we conclude that a more extensive measurement campaign is required to obtain a validation with scanning lidars. To this end, we propose several recommendations for future measurements campaigns with the aim of model validation and wind farm wake analysis.

Acknowledgements
The research was done within the scope of the project LIKE (Lidar Knowledge Europe) H2020-MSCA-ITN-2019, Grant no. 858358, funded by the European Union. The lidar and atmospheric measurements were performed within the research project "OWP Control" (FKZ 0324131A) funded by the German Federal Ministry for Economic Affairs and Energy on the basis of a decision by the German Bundestag. We acknowledge the wind farm operator Global Tech I Offshore Wind GmbH for providing SCADA data and thank them for supporting our work. We would also like to acknowledge our colleagues at ForWind - University of Oldenburg, for their useful feedback and inputs on multiple presentations and internal reviews of the current analysis.

References

[1] Schneemann J, Rott A, Dörenkämper M, Steinfeld G and Kühn M 2020 *Wind Energ. Sci.* **5**(1) 29–49

[2] Hasager C B, Vincent P, Badger J, Badger M, Di Bella A, Peña A, Husson R and Volker P J 2015 *Energies* **8** 5413–5439

[3] Nygaard N G and Newcombe A C 2018 *J. Phys.: Conf. Series* **1037** 072008

[4] Platis A, Siedersleben S K, Bange J, Lampert A, Bärfuss K, Hankers R, Cañadillas B, Foreman R, Schulz-Stellenfleth J, Djath B *et al.* 2018 *Scientific reports* **8** 1–10

[5] Pettas V, Kretschmer M, Clifton A and Cheng P W 2021 *Wind Energ. Sci.* **6** 1455–1472

[6] Nygaard N G, Steen S T, Poulsen L and Pedersen J G 2020 *J. Phys.: Conf. Series* **1618** 062072

[7] Maas O and Raasch S 2022 *Wind Energy Science* **7** 715–739

[8] Cañadillas B, Beckenbauer M, Trujillo J J, Dörenkämper M, Foreman R, Neumann T and Lampert A , in review, 2022 *Wind Energ. Sci. Discuss. [preprint]* 1–29

[9] Porté-Agel F, Bastankhah M and Shamsoddin S 2020 *Boundary-Layer Meteorology* **174** 1–59

[10] Bastankhah M, Welch B L, Martínez-Tossas L A, King J and Fleming P 2021 *J. Fl. Mech.* **911** 53

[11] Katic I, Højstrup J and Jensen N O 1986 *Eur. wind energ. asso. conf. and exh.* **1** 407–410

[12] Beck H and Kühn M 2017 *Remote Sensing* **9**(6)

[13] Werner C 2005 Doppler wind lidar *Lidar* (Springer) pp 325–354

[14] Rott A, Schneemann J, Theuer F, Trujillo Quintero J J and Kühn M , in review, 2021 *Wind Energ. Sci. Discuss.* 1–28

[15] Rodrigo J S, Cantero E, García B, Borbón F, Irigoyen U, Lozano S, Fernande P and Chávez R 2015 *J. Phys.: Conf. Series* **625** 012044

[16] Theuer F, van Dooren M F, von Bremen L and Kühn M 2020 *Wind Energ. Sci.* **5** 1449–1468

[17] Bot E and Kanev S 2020 Farmflow: extensively validated and dedicated model for wind farm control Tech. rep. TNO, Petten, The Netherlands

[18] Schmidt J, Requate N and Vollmer L 2021 *J. Phys.: Conf. Series* **1934** 012020

[19] Bastankhah M and Porté-Agel F 2014 *Renewable energy* **70** 116–123

[20] Crespo A, Herna J *et al.* 1996 *Journal of wind engg. and ind. aerodyn.* **61** 71–85

[21] Jonkman J, Butterfield S, Musial W and Scott G 2009 Definition of a 5-mw reference wind turbine for offshore system development Tech. rep. National Renewable Energy Lab.(NREL), Golden, CO (United States)